## PROCEEDINGS OF SPIE

SPIEDigitalLibrary.org/conference-proceedings-of-spie

# GPI 2.0: performance of upgrades to the Gemini Planet Imager CAL and IFS

Dillon Peng, Maeve Curliss, Mary Anne Limbach, Jeffrey Chilcote, Randall Hamper, et al.

Dillon Peng, Maeve Curliss, Mary Anne Limbach, Jeffrey Chilcote, Randall Hamper, Quinn Konopacky, Joeleff Fitzsimmons, Bruce Macintosh, Christian Marois, Fredrik Rantakyrö, Arlene Aleman, Jérôme Maire, Robert De Rosa, Emiel Por, Dmitry Savransky, Brian Sands, Marshall Perrin, Remi Soummer, Isabel Kain, Laurent Pueyo, Bryony Nickson, Meiji Nguyen, Clarissa Do Ó, Saavidra Perera, Eckhart Spalding, "GPI 2.0: performance of upgrades to the Gemini Planet Imager CAL and IFS," Proc. SPIE 12184, Ground-based and Airborne Instrumentation for Astronomy IX, 1218443 (29 August 2022); doi: 10.1117/12.2630329



Event: SPIE Astronomical Telescopes + Instrumentation, 2022, Montréal, Québec, Canada

### GPI 2.0: Performance of upgrades to the Gemini Planet Imager CAL and IFS

Dillon Peng<sup>a</sup>, Maeve Curliss<sup>b</sup>, Mary Anne Limbach<sup>b</sup>, Jeffrey Chilcote<sup>a</sup>, Randall Hamper<sup>a</sup>, Quinn Konopacky<sup>c</sup>, Joeleff Fitzsimmons<sup>d</sup>, Bruce Macintosh<sup>e</sup>, Christian Marois<sup>d,f</sup>, Fredrik Rantakyrö<sup>g</sup>, Arlene Aleman<sup>e</sup>, Jérôme Maire<sup>c</sup>, Robert De Rosa<sup>h</sup>, Emiel Por<sup>i</sup>, Dmitry Savransky<sup>j</sup>, Brian Sands<sup>a</sup>, Marshall Perrin<sup>i</sup>, Remi Soummer<sup>i</sup>, Isabel Kain<sup>k</sup>, Laurent Pueyo<sup>i</sup>, Bryony Nickson<sup>i</sup>, Meiji Nguyen<sup>i</sup>, Clarissa Do Ó<sup>c</sup>, Saavidra Perera<sup>c</sup>, and Eckhart Spalding<sup>a</sup>

<sup>a</sup>Department of Physics and Astronomy, University of Notre Dame, 225 Nieuwland Science Hall, Notre Dame, IN, 46556, USA

<sup>b</sup>Department of Physics and Astronomy, Texas A&M University, 4242 TAMU, College Station, TX, 77843-4242, USA

<sup>c</sup>Center for Astrophysics and Space Science, University of California San Diego, La Jolla, CA 92093, USA

<sup>d</sup>National Research Council of Canada Herzberg, 5071 West Saanich Road, Victoria, BC V9E2E7, Canada

<sup>e</sup>Kavli Institute for Particle Astrophysics and Cosmology, Stanford University, Stanford, CA 94305, USA

<sup>f</sup>University of Victoria, 3800 Finnerty Road, Victoria, BC, V8P 5C2, Canada <sup>g</sup>Gemini Observatory, Casilla 603, La Serena, Chile

<sup>h</sup>European Southern Observatory, Alonso de Córdova 3107, Vitacura, Santiago, Chile <sup>i</sup>Space Telescope Science Institute, Baltimore, MD 21218, USA

<sup>j</sup>Sibley School of Mechanical and Aerospace Engineering, Cornell University, Ithaca, NY 14853, USA

<sup>k</sup>Department of Astronomy & Astrophysics, University of California Santa Cruz, 1156 High Street, Santa Cruz, CA 95064, USA

#### ABSTRACT

The Gemini Planet Imager (GPI) is a facility class instrument for the Gemini Observatory with the primary goal of directly detecting young Jovian planets. After several years of successful operations on sky at Gemini South, GPI is undergoing maintenance and upgrades at the University of Notre Dame and is being moved to Gemini North. We present the current performance results, from in-lab testing, for several of the upgraded components to the Integral Field Spectrograph (IFS) and the Calibration Wavefront Sensor (CAL) for GPI 2.0. These upgrades include changes to the IFS dispersion prisms, changes to the pupil viewing cameras, and changes to the low order wavefront sensor. These improvements are designed to improve the magnitude and contrast range of GPI. The IFS prism upgrades are expected to provide more equal spectral lengths across the Y, J, H, and K bands, while the new pupil and CAL cameras are expected to outperform their predecessors in several key metrics. We describe the alignment of several components, their noise characteristics, and their performance in the GPI environment.

Keywords: Gemini Planet Imager, exoplanets, instrumentation, wavefront sensor, detectors

Further author information: (Send correspondence to D.P.) D.P.: E-mail: dpeng@nd.edu, Telephone: +1 510 585 8805

Ground-based and Airborne Instrumentation for Astronomy IX, edited by Christopher J. Evans, Julia J. Bryant, Kentaro Motohara, Proc. of SPIE Vol. 12184, 1218443 © 2022 SPIE · 0277-786X · doi: 10.1117/12.2630329

#### 1. INTRODUCTION

As it ends its tenure at Gemini South in Chile, GPI is slated for a handful of upgrades at the University of Notre Dame. The scope of this paper is meant to cover upgrades to two of the major subsystems, the calibration system (CAL) and the integral field spectrograph (IFS). This includes the performance and testing of upgrades to two detectors, a microlens array, and new IFS prism sets. However, due to delays and time constraints, testing of only the detector upgrades for the Shack-Hartmann wavefront sensor and the pupil plane camera have been done. The microlens array has been obtained and is ready for installation in front of the CAL detector once characterization and testing is completed, and the IFS prisms have been received but have not been tested yet. GPI itself has been received at the University of Notre Dame, but is still in the process of being set up. As such, the numerical results of preliminary testing of the detector upgrades will be discussed below, but only qualitative discussion of the microlens array and prisms will be included.

#### 2. OVERVIEW OF THE GPI CAL AND IFS

The infrared wavefront sensor module, or CAL, is a subsystem of GPI that takes light from the focal plane mask (for the low-order wavefront sensor, or LOWFS) and light from the off-axis science beam (for the high-order wavefront sensor, or HOWFS) to detect distortions and aberrations in the incoming wavefront. The CAL is located downstream of the coronagraph, to provide corrections that the adaptive optics (AO) system does not cover. This system was designed to provide feedback for small corrections to incoming wavefronts. To improve its performance, the CAL is will have several upgrades made to it, including a changes in the microlens array and detector of the LOWFS to provide better performance at lower magnitudes. The lenslet array will be mounted to the front of one of the new C-RED 2 cameras using parts custom-machined at the University of Notre Dame, and will be aligned in front of only a specific 96 x 96-pixel area of the detector.

The main science instrument of GPI is the IFS, which is used to take spectra of exoplanets and disks. The major upgrades the IFS is undergoing consists of two new prism sets and filters, with one prism replacing the current prism in the spectrograph and one being added for an entirely new low-resolution mode. In addition to this, the pupil plane camera is also being replaced with a C-RED 2, to allow for better alignment of components within the system.

#### 3. QUALITATIVE OVERVIEW OF UPGRADES

#### 3.1 Detector Upgrades

The cameras for both the CAL and the IFS are being upgraded, from Goodrich SU320KTX-1.7 RT cameras to the much newer and improved First Light Imaging C-RED 2 cameras. Table 1 below details some of the technical improvements that the C-RED 2s bring over the Goodrich cameras, notably including a much higher FPS (frames per second), variable gain settings, and a correlated double sampling (CDS) recording mode.

Table 1. Technical comparison of the detector upgrades from GPI 1.0 (left) and GPI 2.0 (right) for the CAL LOWFS and IFS pupil plane camera.

	SU320KTX-1.7RT	C-RED 2
Pixel pitch $(\mu \text{ m})$	40	15
Plane size (pixels)	$320 \times 240$	$640 \times 512$
Full Frame Read noise $(e^-)$	< 50	< 30
Max FPS (full area)	72	600
Non-destructive readout	No	Yes
Variable gain modes	No	Yes

While the full area FPS of the C-RED 2 is limited to 600 frames per second, only a 96 by 96 pixel area will actually be used by the CAL; running in this limited area mode, an FPS of over 4000 can be achieved. For

GPI 2.0, two C-RED 2 cameras were obtained. Because only a small area of the plane is necessary for the CAL camera, as opposed to the entire area being used for the IFS pupil plane camera, the camera with an overall higher variation in sensitivity was chosen to be used for the CAL, while the other was chosen for use in the pupil plane. The area on the CAL camera to be used was then chosen by finding the area with the lowest average noise.



Figure 1. One of the new C-RED 2 cameras that will be installed in GPI 2.0.

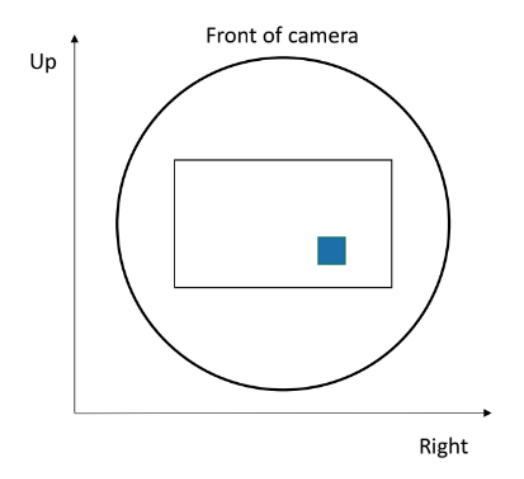


Figure 2. The optimal location to position the microlens array over the CAL C-RED 2, as determined by Maeve Curliss. This region lies at a position of 0.084 - 0.228 cm up and 0.672 - 0.816 cm right from the bottom left of the detector (facing it), which translates to a pixel range of [360 - 455] in the x and [448 - 543] in the y-direction.

#### 3.2 Microlens Array Upgrade

The lenslet array used in the LOWFS of GPI 1.0 is a OKO APO-P(GB)-P200, and is being replaced with a Newport MALS-11 Microlens Array. A comparison of the technical specifications of the two can be seen in Table 2 below; the MALS-11 was chosen due to its relative similarity and ease of integration into the instrument relative to the previous microlens array over other options while still providing improvements in performance; for example, there were other options considered which would have required a change in the relay optics, or removal of relay optics altogether. A major difference between the two, however, is the pixel pitch; with a pixel pitch

of 300  $\mu$ m, the MALS11 can line up with an integer number of pixels on the C-RED 2 detector, which has a pixel pitch of 15  $\mu$ m. This allows for effective quad-cell computing for the Shack-Hartmann Wavefront Sensor (SHWFS), allowing for faster calculations for alignment over Gaussian fitting. The lenslet array holder has been designed and machined at the University of Notre Dame, but has yet to be fitted onto the C-RED 2 with the lenslet array itself within it.

Table 2. Technical comparison of the microlens array changes from GPI 1.0 (left) and GPI 2.0 (right) for the CAL LOWFS. The MALS11 provides a balance of improvement in terms of performance and similarity to the previous configuration.

	OKO APO-P(GB)-P200	Newport MALS11
Material	BK-7/NOA-61	UV Grade Fused Silica
Size (mm)	$15 \times 15$	$10 \times 10$
Lenslet pitch $(\mu m)$	200	300
Lenslet focal length at 633 nm (mm)	6.4	8.7
Lenslet focal length at 1.6 $\mu m$ (mm)	6.6	9.0

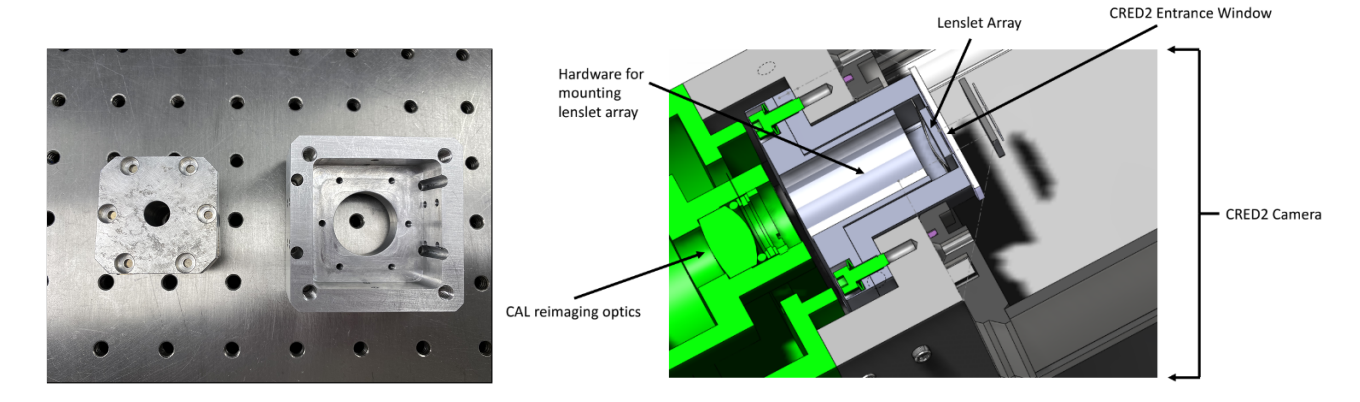


Figure 3. The machined parts made for holding the microlens array in place in front of the C-RED 2 (left), and a CAD diagram of the microlens array holder in place in front of the C-RED 2 (right).

#### 3.3 IFS Prism Upgrades

The major upgrades the IFS is undergoing consists of two new prisms, with one replacing the current prism in the spectrograph and one being added for an entirely new low-resolution mode. Originally, GPI 1.0 has a single prism, with separate band-passes for the Y, J, H, K1, and K2 bands, with the K-band being split to be able to fit the entire spectral range on the detector. With the new prisms, the K1 and K2 bands are consolidated back into a singular band with slightly lower resolution. The original prism is made of S-FTM16/BaF2 material, while the new ones are made of N-SF66/CaF2. The new prisms provide better resolution over the wavelengths GPI 2.0 will be observing at, and also provides a more even spectral resolution over the entire wavelength band. This uniformity is what allows for the implementation of the low-resolution mode, which will be able to observe over the Y, J, H, and K bands simultaneously. Below are Tables 2 and 3, which detail the wavelength cutoffs, pixel lengths (on the detector), and resolutions of the different observing bands for the high and low-resolution modes, respectively.

See [1] for an in-depth overview of the IFS improvements from GPI 1.0 to GPI 2.0. Further decisions in refinement and optimization have resulted in a change to the current material selections of the prisms, but the reasoning and expected performance improvements behind the upgrades are still relevant. Additionally, there is further discussion about the properties of the new filters, which are not covered in this paper.

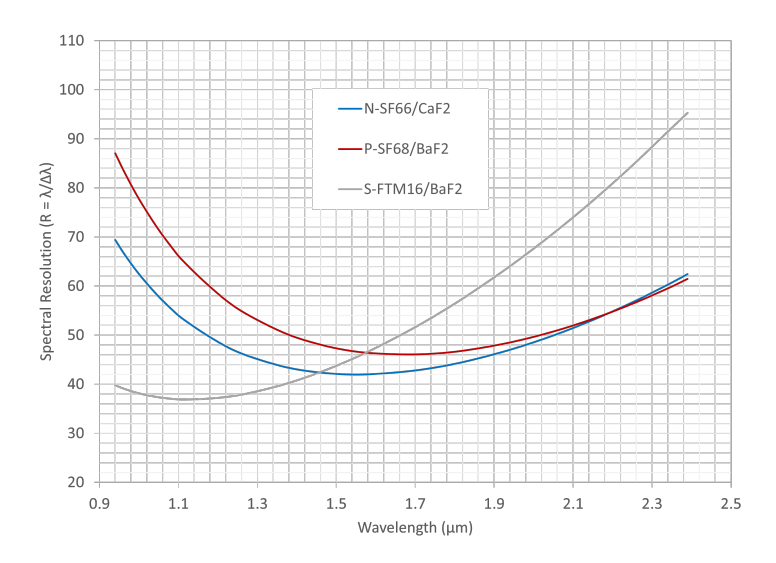


Figure 4. Comparison of spectral resolutions at different wavelengths of prisms of different materials considered for the IFS upgrade. The performance of the previous material from GPI 1.0 is shown in grey, while the performance of prisms for GPI 2.0 are shown in blue. Note the more even spectral resolution of the new N-SF66/CaF2 materials.

Table 3. Table displaying the cut-on/cut-off wavelengths for the different bands of the new prisms in the high-resolution mode, as well as their pixel widths on the detector along with their spectral resolutions.

	Cut-on/Cut-off (m)	Length (pix)	$R = \lambda/\Delta\lambda$
y-band:	0.950 - 1.070	14.7	61.9
J-band:	1.121 - 1.346	17.5	47.9
H-band:	1.498 - 1.796	15.4	42.7
K-band:	2.000 - 2.400	20.0	55.1

Table 4. Table displaying the cut-on/cut-off wavelengths for the different bands of the new prisms in the new low-resolution mode, as well as their pixel widths on the detector along with their spectral resolutions. Because all bands will be observed simultaneously in this mode, there are gaps between them that are several pixels in length as well. Note the more uniform spectral resolutions across the wavelengths in this mode.

	Cut-on/Cut-off (m)	Length (pix)	$R = \lambda/\Delta\lambda$
y-band:	0.97 - 1.07	2.7	13.6
Gap:		2.1	
J-band:	1.17 - 1.33	2.7	10.5
Gap:		2.2	
H-band:	1.49 - 1.78	3.4	9.6
Gap:		2.4	
K-band:	2.00 - 2.40	4.5	12.4

#### 4. DETECTOR TESTING AND ANALYSIS

The C-RED 2s were tested in a clean room under GPI 2.0 running conditions, with the detector cooled to -40 degrees Celsius. A Thorlabs OSL2 Fiber Illuminator was used as a broadband light source, and fed into a Newport 819D-IS-5.3 PTFE Integrating Sphere to provide diffuse light for detector characterization (without filters). Frames were taken at a variety of integration times to cover a large range of detector saturation, using the full detector size for the pupil plane and the specified region for the LOWFS. Corresponding dark frames at the same integration times and flat-field images were taken as well.

The C-RED 2 uses a 14-bit A/D converter; when taking frames, an effort was made to cover as wide as a range of values as possible in order to measure noise, linearity, and gain across the saturation level of the detector, ranging from around 2000 counts to 15000 counts. Below are results of the testing; included are values obtained for the average noise values and standard deviation of pixel values for dark frames, along with estimations of the gain value and linearity of the detector at different gain levels.

Gain was calculated using a simple linear polynomial fit of a linear portion of the signal to noise data, as seen in Figure 6. Ideally, Equation 1 (Equation 9.10 from [2]) would be used, where  $V_m$  is the variance (noise squared),  $S_m$  is the mean (signal), g is the gain, and R is the readout noise. However, attempting to fit the points to that form of equation resulted in the y-intercept being negative, corresponding to a negative readout noise. More data will be taken and analyzed in the linear regions of signal to noise found in an attempt to calculate a more accurate gain value.

$$V_m = \frac{1}{g}S_m + (\frac{R}{g})^2 \tag{1}$$

There are currently two main noticeable issues regarding the detectors. The first is that there is a clear pattern of light/dark columns on the detectors, as seen in the dark frame, of Figure 5. The second is that frames taken in the ROI mode occasionally had a strange pattern in which the top row of pixels were relatively unsaturated or completely "0" compared to the rest of the detector; the cause of this behavior is currently unknown. Because the outer edges of the ROI are unnecessary for the SHWFS, a one-pixel border was stripped away for the analysis of the CAL camera.

Some less obvious troubles lie in strange outlier behaviors regarding the noise values at different integration times; in almost all of the tests conducted, there were 2 - 3 integration times per gain setting where the average noise value was much higher (or lower) than at other integration times, with no apparent pattern. Further data collection and analysis will be done to try to pinpoint the source of these issues.

Table 5. Values obtained from analysis of the CAL camera in the  $96 \times 96$  region of interest at all 3 different gain values.

	Low Gain	Medium Gain	High Gain
Mean Dark Value (ADU)	741.52	463.64	696.33
Gain	14.27	15.00	3.75
StDev of Residuals	5.83	14.50	37.01

Table 6. Values obtained from analysis of the IFS camera in the full frame at all 3 different gain values.

	Low Gain	Medium Gain	High Gain
Mean Dark Value (ADU)	811.34	709.29	861.97
Gain	7.14	1.9	0.91
StDev of Residuals	10.78	5.81	359.28

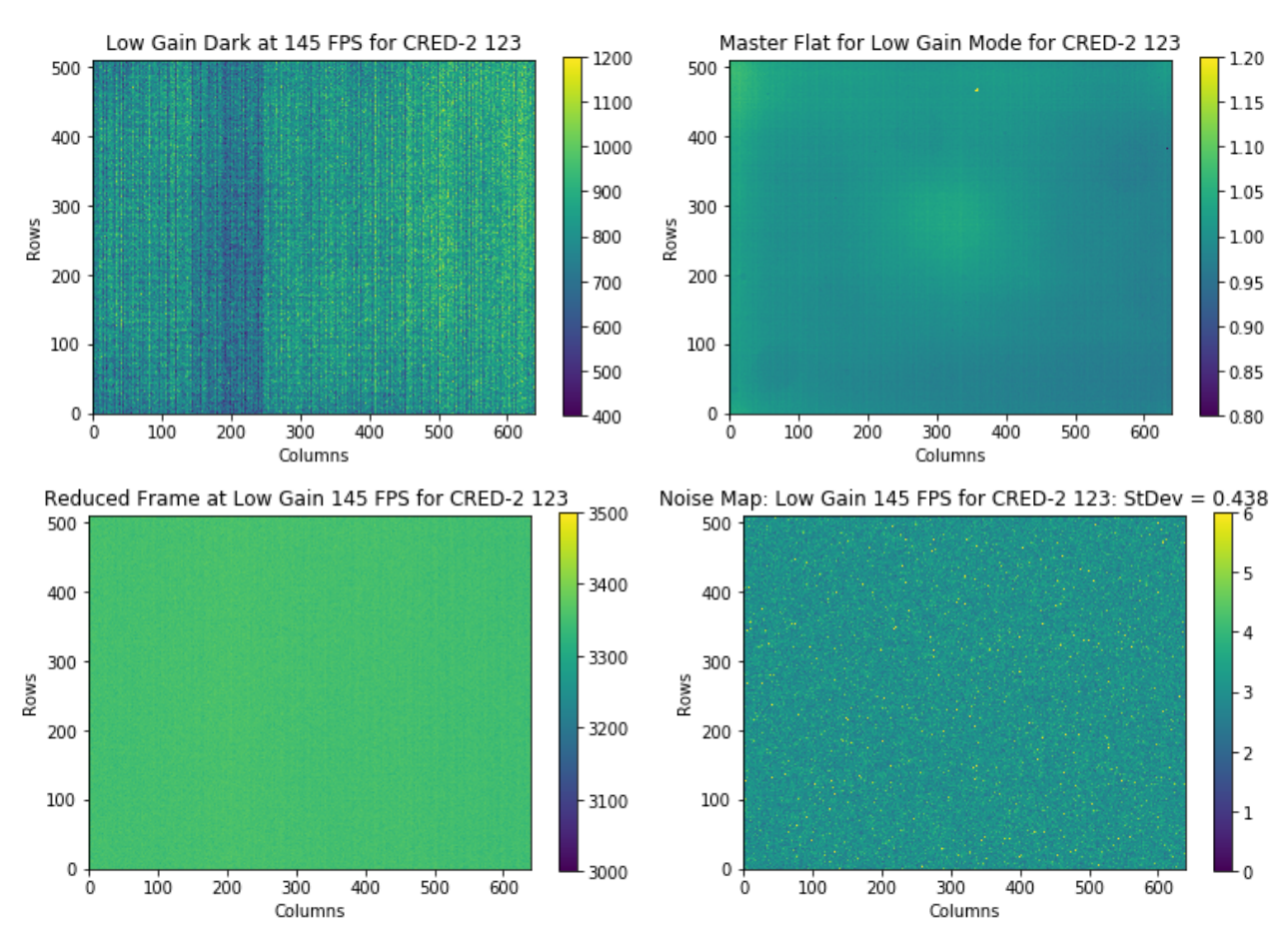


Figure 5. Examples of data frames and reductions applied to analyze and characterize the detector behavior. These particular images show the dark, flat, final reduced frame (of a diffusely illuminated image), and noise map at a certain integration time for the Low Gain mode of the IFS camera in full frame mode. The units are all in ADU, except for the flat image, which was normalized (unitless) to show sensitivity per pixel.

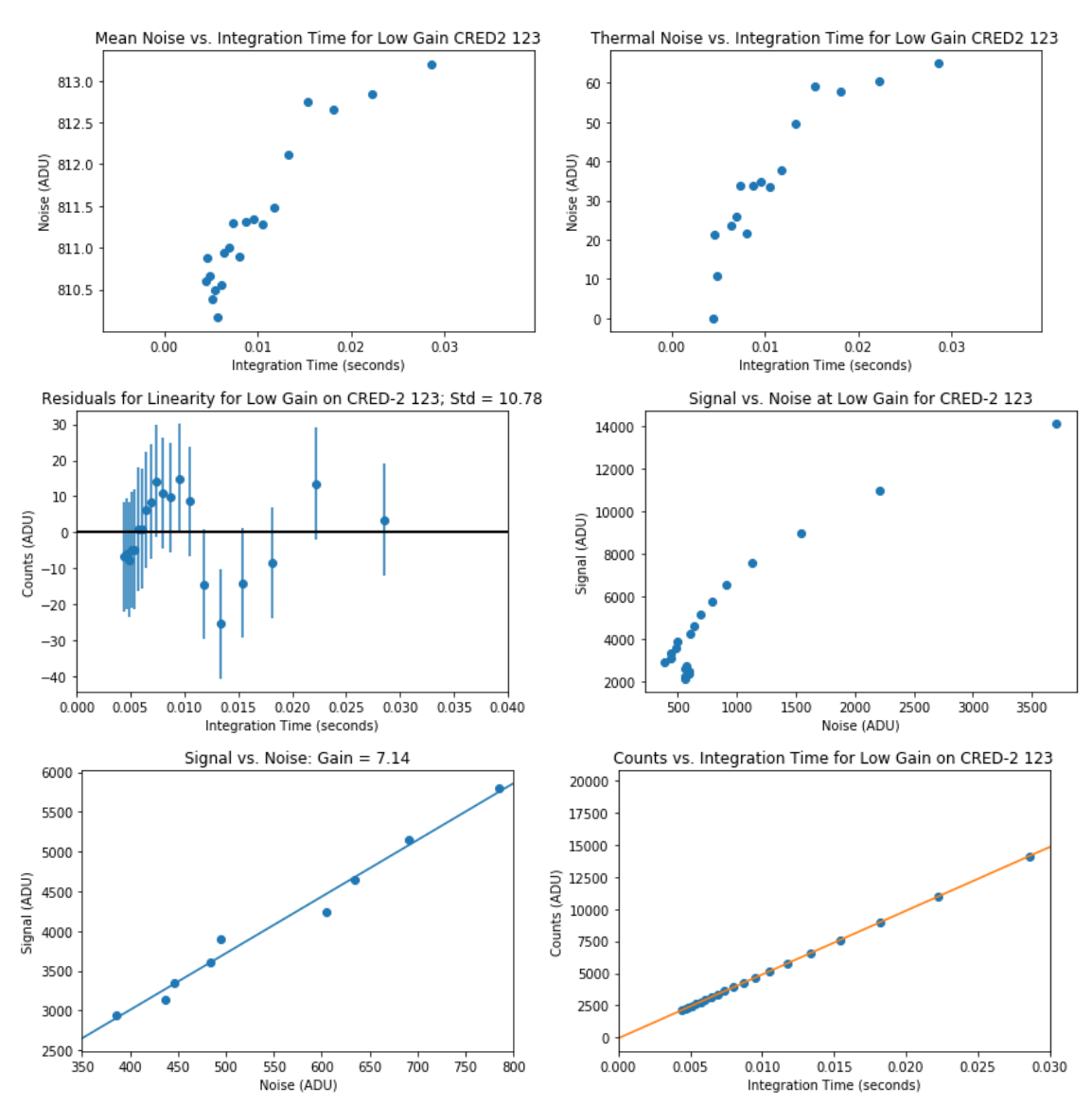


Figure 6. Example plots showing the trends and analysis of the IFS camera in full frame mode at Low Gain. Calculations like these were made for each camera at in each of the three gain modes. The second plot in the second row is shown to demonstrate the signal vs. noise across the entire saturation level, as opposed to the linear region which was used to calculate the gain in the first figure in the third row.

#### 5. CONCLUSION

Extensive testing and analysis is still required to fully characterize the behavior and performance of the upgrades to the GPI CAL and IFS systems. Due to delays, the IFS prisms have not arrived yet, so no data about their performance can be gathered. The lenslet array is yet to be installed in front of the new CAL C-RED 2 as well, so there is currently no data to report on that as well.

The First Light Imaging C-RED 2 cameras have undergone some testing, but require more in order to properly understand some of the strange behavior observed. Generally, more data should be taken in order to determine the cause of inconsistencies in noise levels at different integration times, and to attempt to explain the light/dark column patterns observed in the darks. Specifically, more data should be taken in the linear regimes of the detectors in order to obtain more robust gain values. Gibson et al. 2019 [3] provides some techniques used in characterizing a C-RED 2 detector that may be referenced as well.

#### ACKNOWLEDGMENTS

The GPI 2.0 project is supported by a NSF-MRI grant (award AST-1920180) and the Heising-Simons Foundation. The original GPI was supported by NSF grants AST-1411868 and AST-1518332. The international Gemini Observatory is a program of NSF's NOIRLab, which is managed by the Association of Universities for Research in Astronomy (AURA) under a cooperative agreement with the National Science Foundation. on behalf of the Gemini Observatory partnership: the National Science Foundation (United States), National Research Council (Canada), Agencia Nacional de Investigación y Desarrollo (Chile), Ministerio de Ciencia, Tecnologíae Innovación (Argentina), Ministério da Ciência, Tecnologia, Inovações e Comunicações (Brazil), and Korea Astronomy and Space Science Institute (Republic of Korea).

#### REFERENCES

- [1] Limbach, M. A., Chilcote, J., Konopacky, Q., Rosa, R. D., Hamper, R., Macintosh, B., Marois, C., Perrin, M., Savransky, D., Veran, J.-P., Wang, J., and Aleman, A., "GPI 2.0: Upgrades to the IFS including new spectral modes," in [Ground-based and Airborne Instrumentation for Astronomy VIII], Evans, C. J., Bryant, J. J., and Motohara, K., eds., 11447, 1127 1134, International Society for Optics and Photonics, SPIE (2020).
- [2] McLean, I. S., [Electronic Imaging in Astronomy: Detectors and Instrumentation (Second Edition)], Praxis Publishing Ltd, Chichester, UK, second ed. (2008).
- [3] Gibson, R. K., Oppenheimer, R., Matthews, C. T., and Vasisht, G., "Characterization of the C-RED 2: a high-frame rate near-infrared camera," *Journal of Astronomical Telescopes, Instruments, and Systems* **6**(1), 1 9 (2019).